Microfluidics

International Edition: DOI: 10.1002/anie.201911252
German Edition: DOI: 10.1002/ange.201911252

Controllable Synthesis of Multicompartmental Particles Using 3D Microfluidics

Zengnan Wu, Yajing Zheng, Ling Lin, Sifeng Mao, Zenghe Li, and Jin-Ming Lin**

Abstract: *A microfluidic assembly method based on a microfluidic chip and capillary device was developed to create multicompartmental particles. The microfluidic chip design endows the particles with regulable internal structure. By adjusting the microstructure of the chip, the diameter of the capillary, the gap length between the two microfluidic components, and the flow rates, the size of the particles and the number or the ratio of different regions within the particle could be widely varied. As a proof of concept, we have produced some complicated particles that even contain 20 compartments. Furthermore, the potential applications of the anisotropic particles are explored by encapsulating magnetic beads, fluorescent nanoparticles, and the cells into different compartments of the microparticles. We believe that this method will open new avenues for the design and application of multicompartmental particles.*

Inspired by the compartmental structure and positional assembly in eukaryotic cells, configuring multipurpose heterogeneous hydrogel materials into a multicompartmental particle has received extensive attention in biomedical applications.[1] These higher-order assemblies with anisotropic modifications have been used for various applications, such as the loading of multiple drugs,[2] hierarchical delivery,[3] intelligent sensors,[4] and controllable movement.[5] Furthermore, precise spatial arrangement immensely increases the design parameter space of the assembly of cells and biomaterials, which allows us to profoundly understand the interplay between physical and biological properties.[6]

Diverse fabrication methods have been recently suggested, but it is still challenging to construct a multiscale, hierarchical, branching unit. For example, the planar microfluidic-chip-assisted approaches are restricted to the production of particles with a parallel arrangement of compartments on account of the two-dimensional co-flowing streams.[7] The coaxial capillary microfluidic system and the centrifugation-based method extend the diversity in geometry but are limited by poor pattern controllability.[8] Flow lithography techniques increase the morphology complexity, whereas the adjustment of internal compartmental architecture is still difficult to achieve.[9] Furthermore, electrohydrodynamic co-jetting can produce nanometer-size particles, but it is not suitable for producing monodisperse multicompartmental particles.[10]

Herein, we report a vertical integrated chip–capillary droplet generator (ICCDG, Figure 1 a). The upstream microfluidic chip, used for driving and configuring multiphase liquids into the system, is devoted to defining the internal microstructure of the particles. The downstream capillary-based device, used as the classic flow-focusing model, is intended to produce ideal spherical hydrogel particles. This powerful microfluidic technique has a flexible design and is simple to produce, so that other than dual-, six-compartment compositions mentioned in previous work,[8b] we easily proceed ten-, even twenty-compartment particles. To our knowledge, this is the first report of such results. Furthermore, by encapsulating magnetic beads, fluorescent nanoparticles, and various cell lines, more functions including cell coding, were demonstrated and the potential applications of multicompartmental particles were shown.

The ICCDG system including an upstream horizontal microfluidic chip and a downstream vertical capillary-based device is detailed in Figure S1 in the Supporting Information.

[*] Z. N. Wu, Prof. Z. H. Li
State Key Laboratory of Chemical Resource Engineering, Beijing University of Chemical Technology, Beijing 100029 (China)
Z. N. Wu, Y. J. Zheng, Dr. S. F. Mao, Prof. J.-M. Lin
Department of Chemistry, Beijing Key Laboratory of Microanalytical Methods and Instrumentation, MOE Key Laboratory of Bioorganic Phosphorus Chemistry & Chemical Biology, Tsinghua University
Beijing 100084 (China)
E-mail: jmlin@mail.tsinghua.edu.cn
Z. N. Wu, Y. J. Zheng, Dr. L. Lin
CAS Key Laboratory of Standardization and Measurement for Nanotechnology, CAS Center for Excellence in Nanoscience, National Center for Nanoscience and Technology
Beijing 100190 (China)
E-mail: linling@nanoctr.cn
Supporting information and the ORCID identification number(s) for the author(s) of this article can be found under: https://doi.org/10.1002/anie.201911252.

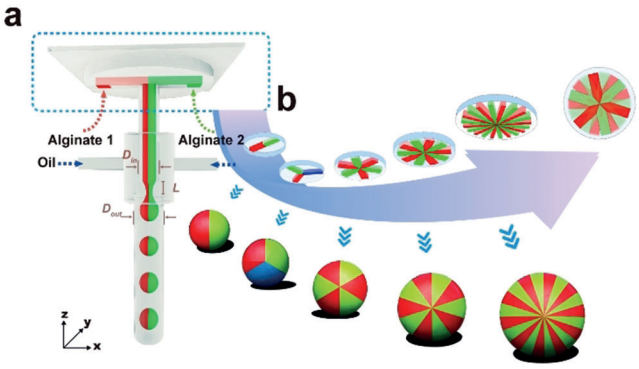

Figure 1. The integrated chip–capillary droplet generator (ICCDG). a) Schematic illustration of the ICCDG for producing the dual-compartment particles. b) The multicompartmental particles that were obtained from the ICCDG system equipped with corresponding upstream chips.

The microfluidic chip consists of a set of channels, which are symmetrically distributed around one vertical outlet. The capillary-based device is mainly constructed from an input capillary, an auxiliary capillary, a four-way valve, and an output capillary. In the particle-fabrication experiment, multiple alginates were pumped into the injection channel and converged at the outlet of the chip. Upon exiting the chip, they formed a cluster of vertical laminar co-flows inside the input capillary. When they flowed out of the input capillary, they were focused on the central axis by injecting immiscible acidified oil and were broken up into microdroplets inside the output capillary. Meanwhile, the acetic acid diffused into droplets and triggered rapid in situ crosslinking of Ca-alginate. In the ICCDG system, the flexible design of the upstream chip consists of multiple microchannels resembling a pie chart with arbitrary central angles, which results in the production of hydrogels with different cross-sectional patterns (Figure 1b). In brief, the microconfiguration of the multiple flows determines the three-dimensional structure of the particles. The arrangement of microchannels can endow particles various numbers of compartments. Furthermore, facilitated by the vertical coaxial configuration, the alginate dispersed phase is surrounded entirely by coaxial oil stream at the joint of two immiscible flows, which prevents the dispersed phase from wetting the channel walls.[11] Thus, it avoids hydrogel collapse by producing the droplets one-by-one along the centerline of the channel. Such a unique combination of the microfluidic system extends a novel approach for controllable fabrication of anisotropic particles.

To fabricate multicompartmental particles, we obtained the dual-compartment particles from the two-channel microfluidic device. The morphology and diameter distribution of particles was obtained from confocal microscopy (Figure 2a,b). The low coefficient of variation of the diameter (approximately 2%) indicates that the ICCDG is able to produce highly monodispersed droplets. Furthermore, we examined the relationship between the particle properties and the device parameters. The particle size is controllable by adjusting the ratio of the oil (Q_{oil}) and Ca-alginate (Q_{alg}) flow rates (Q_{oil}/Q_{alg}), the distance (L) between the two capillaries as well as the diameter of the capillary (D_{in} and D_{out}). For a certain device ($L = 200$ μm, D_{in} 250 μm, and $D_{out} = 400$ μm), the microdroplet size decreases as the flow-rate ratio (Q_{oil}/Q_{alg}) increases (Figure 2c). The diameter can be increased by simply lengthening the distance L when D_{out}, Q_{oil}, and Q_{alg} are fixed (Figure 2d). Furthermore, it was found that the microdroplet size increases in direct proportion to the value of D_{out} (Figure 2e). Consequently, a large size-distribution range of droplet diameter could be achieved by the coordinated adjustment of various parameters. Notably, the effect of diffusive mixing and convective transport on the interstructure of droplets during droplet formation are worth considering. In the co-flow stream, because of low Reynolds numbers, there is no obvious diffusive mixing among the flow streams in the microscale capillary channel (Supporting Information, Figure S2). In a typical flow-focusing model, the unavoidable shear stresses will exacerbate the convective transport. However, rapid diffusion-controlled Ca-alginate gelation can eliminate this effect, causing an extremely sharp

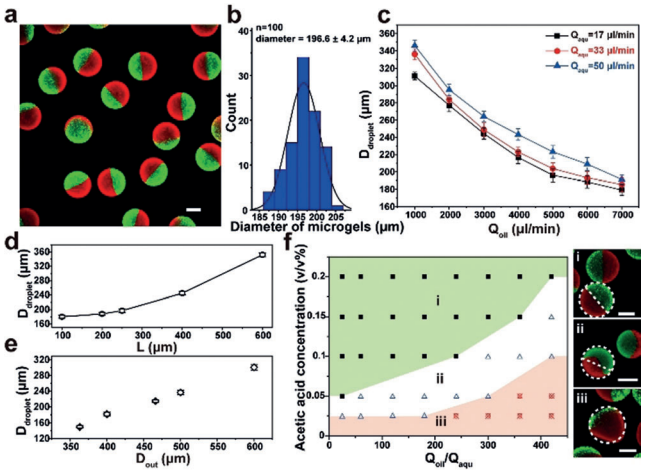

Figure 2. The effect of fabrication parameters on stable multicompartmental particles. a) Images of dual-compartment particles obtained from the ICCDG. b) Corresponding size distribution of the monodisperse particles. c) Relationship between the diameter of the droplets and flow rates of oil. d) The dependence of the diameter of the droplets ($D_{droplet}$) on the length between the inlet and outlet capillaries (L), and e) the diameter of outlet (D_{out}). Alginate flow rates of 17, 33, and 50 μL min^{-1} were tested. f) Optimal acetic acid concentration and flow-rate ratio Q_{oil}/Q_{alg} for the stable formation of multicompartmental particles. Crosssectional images of i) dual-compartment particles with clear compartmental separations, ii) dual-compartment particles with disturbed compartmental separations, and iii) non-compartment particles, corresponding to the different conditions in (f). Scale bars = 100 μm.

boundary between the two compartments. The stability of the adjacent compartment boundary is of great importance for strict compartmental division. Therefore, we further studied the relationship between the internal architecture of the particle and the acetic acid concentration (Figure 2f). The formation of the distinct interface is affected by the concentration of acetic acid, with a higher concentration (greater than 0.15%) leading to microparticles with a well-defined substructure. A decrease in the concentration of acetic acid (greater than 0.1%) disturbs the separatrix, which presents a slight mixing between adjacent compartments. A lower concentration of acetic acid (less than 0.05%) results in broken spheroids, affecting the mechanical property of the hydrogel particles. Base on this droplet-production process, we speculate that the other types of rapidly gelling materials, such as photopolymerization material (poly(ethylene glycol) diacrylate) and thermal-crosslinking material (poly(N-isopropylacrylamide)/poly(ethylene glycol)), could also be applied in our system.[12]

For the generation of particles with higher numbers of compartments in the ICCDG, the key point is the feasibility and flexibility of flow manipulation in the geometric microchannels. As a proof of our concept, six-, ten-, and twenty-channel microfluidic devices were used as the shaping molds. The corresponding multiple alginate solutions mixed with different fluorescent polystyrene nanoparticles were simultaneously pumped into the injection channels. Similar to the formation process of the dual-compartment particles, six-, ten-, and twenty-compartment particles are finally achieved,

as shown in Figure 3. As predicted, the internal substructure of the particles possessed the ideal geometries resulting from the chip microstructures. The apparent symmetry of the separatrix was unaffected by the increasing number of compartments, which suggested that our approach, in principle, can produce more complex compartmentalization by adjusting the architecture of the device. Compared with the current technologies, our approach produces particles with a higher number of compartments.[1c,8a,b,13] This fluid-manipulation method is beneficial for inspiring the production of more complex particles.

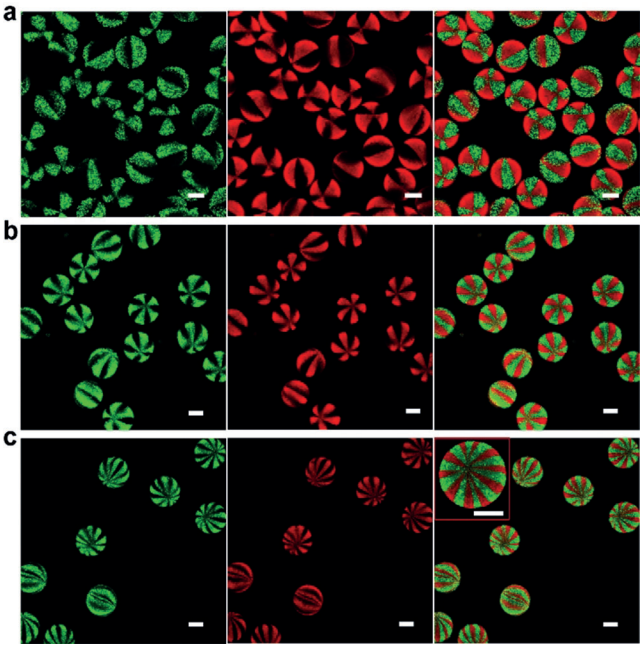

Figure 3. Multicompartmental particles possessing axial symmetry. a) Six-compartment particles obtained from a six-channel microfluidic device. b) Ten-compartment particles obtained from a ten-channel microfluidic device. c) twenty-compartment particles obtained from a twenty-channel microfluidic device. Scale bars = 100 μm. Green = green polystyrene nanoparticles; red = red polystyrene nanoparticles.

Encouraged by the complex hierarchical substructure of the particle, anisotropic materials were encapsulated inside to integrate diverse functions and for applications in the field of biological analysis. Here, fluorescent nanoparticles, magnetic beads, HUVEC cells, and HepG2 cells were dispersed into alginate solutions and the mixtures were injected into the microfluidic device to generate multifunctional particles (Figure 4a). Indeed, the particles displayed a high shape uniformity and clear compartment formation, illustrating that the slight difference of material properties do not influence the compartment framework (Supporting Information, Figure S3).

Interestingly, we noticed that the orientation of the different compartments was essential for positioning and identifying each unit within a particle. The combination of a fluorescent-nanoparticle compartment and magnetic-bead compartment was used to determine the particle orientation. Then the two HUVEC- and HepG2-laden units were arranged clockwise according to the particle orientation. To examine the feasibility of our design, light-sheet fluorescence microscopy (LSFM) was used to visualize the internal microstructure of the particles (Figure 4b and Supporting Information, Movie S1). Firstly, the region of the blue fluorescent nanoparticles was viewed under a fluorescence field, which occupied exactly one-sixth of a sphere (Figure 4bi). Therefore, the remaining five compartments could be divided readily based on the proportion of the fluorescent portion (see the Supporting Information). Then, based on the above partitioning operation, by comparing the orientation of the unknown units relative to the fluorescent nanoparticles and magnetic beads, all the cell-laden units could be identified (Figure 4biii and iv), the green HUVEC-laden unit and the red HepG2-laden unit arranged clockwise according to the particle orientation. Note that, this highly accurate and ordered spatial arrangement could enable the recognition of different cell lines inside one particle without invasive fluorescence labeling.

Furthermore, the particles containing magnetic beads could be actuated by an external magnetic field. It was found that the particle rotates clockwise when turning the magnetic field clockwise around the *z*-axis (Figure 4c), and move in a straight line when the magnetic field was fixed along the *x*- or *y*-axis direction (Figure 4d and Supporting Information, Movie S2). Thus, a noninvasive magnetic force could actuate microparticles to enable the performance of demanding tasks with remote and precise guidance, and fuel-free microswimmers play a critical role in targeted therapy and microrheological probes.[14]

To further demonstrate the potential of the composite microparticle in 3D cell coculturing, unlabeled HUVEC and HepG2 cells were arranged in a multicompartmental particle. We clearly partitioned and identified the cell-laden units in the particle. This non-biolabeling coding method preserves the original cellular phenotype, which is essential for exploring cell behavior with additional tools, such as fluorescence. Hence, after staining with a Calcein AM/EthD-1 kit, we were able to independently monitor the morphology and bioactivity of HUVEC cells and HepG2 cells (Figure 4e and Supporting Information, Figure S4 and Movie S3). Benefitting from the superior compartment structure, the hydrogel particle units possess high compatibility and the encapsulated cells exhibit more than 90% viability during 5 days of culturing (Figure 4f). Although there are no obvious biological phenomenon differences be captured at present, it is foreseeable that such a powerful tool could enable site-specific cellular multiscale analysis, including population studies, spheroid studies, and single-cell studies.

In summary, our anisotropic-particle synthesis method, based on the assembly of a microfluidic chip and capillary, combines the advantages of both the architectural complexity of the microfluidic chip and the high controllability of the capillary. The design could map the plane divergent multiflows to the 3D structure of particles to create well-divided multicompartmental particles. The power of our device was exemplified by the construction of dual-, six-, ten-, and twenty-compartment particles. The primary application was the introduction of a fluorescent-nanoparticle-containing

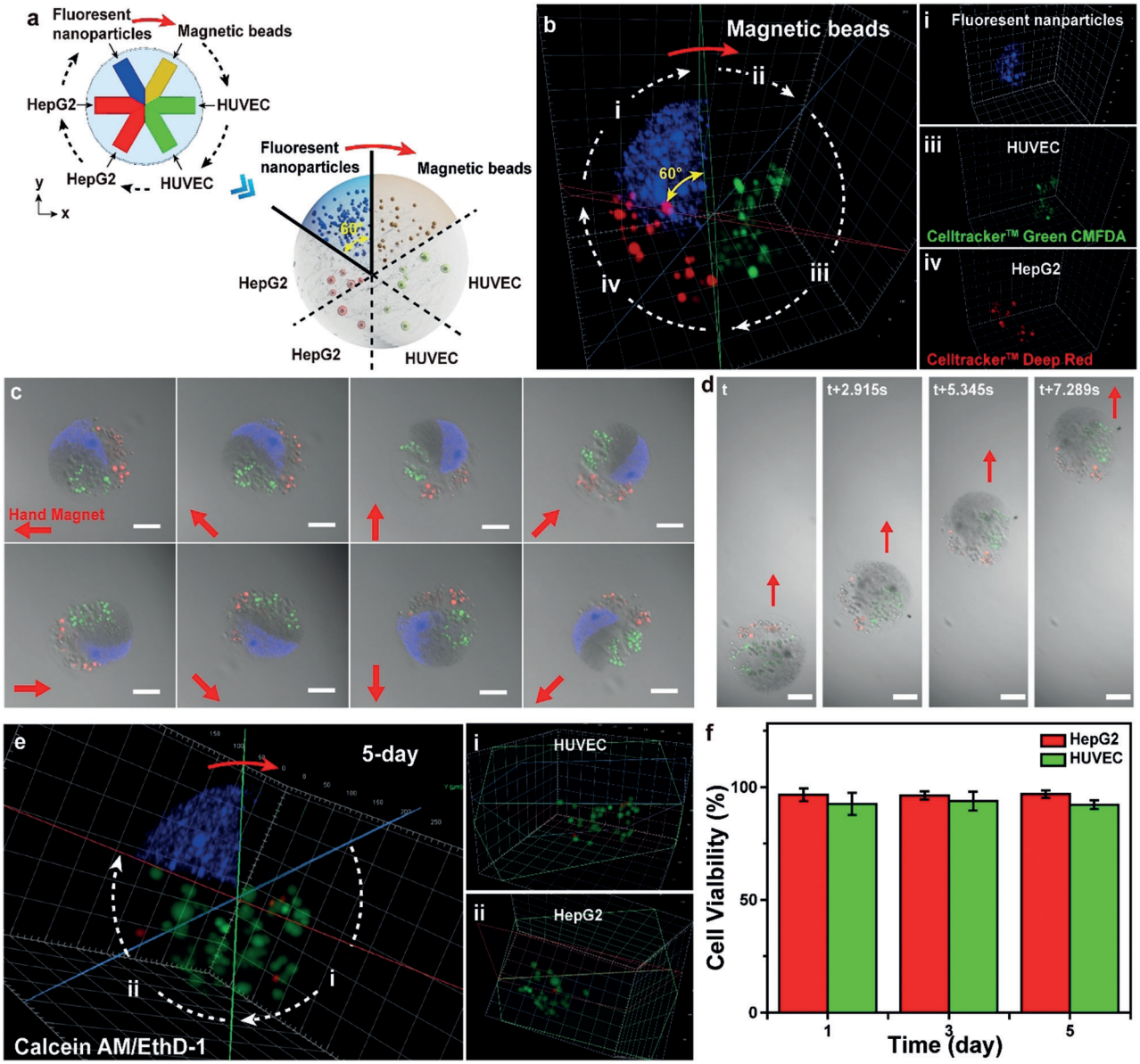

Figure 4. The design and performance of multifunctional particles. a) Schematic illustration of the multifunctional particles and the ordered injection channels for corresponding functional materials. b) Spatial segmentation of particles. Tracking individual functional regions of adjacent compartments within the particle: i) fluoresent nanoparticles, ii) magnetic beads, iii) HUVEC cells labeled using green cell tracker, and iv) HepG2 cells labeled using red cell tracker. c) The rotational motion of particles in response to the magnet, and d) the translational motion of particles in response to the magnet. e) Cell-growth tracking in particles for 5 days. 3D segmentation of different cell lines at 5 days. The viability of i) HUVEC cells and ii) HepG2 cells. f) Results of the cell-growth tracking in (e). Cell viability is characterized by the Calcein AM/Ethd-1 staining kit. Scale bars = 100 μm.

compartment into a multicompartmental particle to encode unmarked units. Furthermore, cells from different cell lines could be encapsulated in different compartments of hydrogel particles and the activity of these different encapsulated cell lines could be monitored simultaneously. Furthermore, other types of cells and materials could also be encapsulated in these hydrogels, thus we expect that the proposed strategy could be considered as a burgeoning approach in the context of cell carrier, particle assembly, and drug screening.[1b]

Acknowledgements

This work was financially supported by National Natural Science Foundation of China (Nos. 21804026, 21727814, and 21435002).

Conflict of interest

The authors declare no conflict of interest.

Keywords: cell encapsulation · fluorescence · hydrogels · microfluidics · multicompartmental particles

[1] a) W. Li, L. Y. Zhang, X. H. Ge, B. Y. Xu, W. X. Zhang, L. L. Qu, C. H. Choi, J. H. Xu, A. Zhang, H. M. Lee, D. A. Weitz, *Chem. Soc. Rev.* **2018**, *47*, 5646 – 5683; b) A. Choi, K. D. Seo, D. W. Kim, B. C. Kim, D. S. Kim, *Lab Chip* **2017**, *17*, 591 – 613; c) L. Y. Zhang, K. W. Chen, H. Y. Zhang, B. Pang, C. H. Choi, A. S. Mao, H. B. Liao, S. Utech, D. J. Mooney, H. N. Wang, D. A. Weitz, *Small* **2018**, *14*, 1702955.

[2] a) B. Herranz-Blanco, L. R. Arriaga, E. Makila, A. Correia, N. Shrestha, S. Mirza, D. A. Weitz, J. Salonen, J. Hirvonen, H. A. Santos, *Lab Chip* **2014**, *14*, 1083 – 1086; b) P. Majumder, U. Baxa, S. T. R. Walsh, J. P. Schneider, *Angew. Chem. Int. Ed.* **2018**, *57*, 15040 – 15044; *Angew. Chem.* **2018**, *130*, 15260 – 15264.

[3] F. He, W. Wang, X. H. He, X. L. Yang, M. Li, R. Xie, X. J. Ju, Z. Liu, L. Y. Chu, *ACS Appl. Mater. Interfaces* **2016**, *8*, 8743 – 8754.

[4] Y. D. Hu, J. Y. Wang, H. Wang, Q. Wang, J. T. Zhu, Y. J. Yang, *Langmuir* **2012**, *28*, 17186 – 17192.

[5] Y. R. Yu, L. R. Shang, W. Gao, Z. Zhao, H. Wang, Y. J. Zhao, *Angew. Chem. Int. Ed.* **2017**, *56*, 12127 – 12131; *Angew. Chem.* **2017**, *129*, 12295 – 12299.

[6] a) B. Grigoryan, S. J. Paulsen, D. C. Corbett, D. W. Sazer, C. L. Fortin, A. J. Zaita, P. T. Greenfield, N. J. Calafat, J. P. Gounley, A. H. Ta, F. Johansson, A. Randles, J. E. Rosenkrantz, J. D. Louis-Rosenberg, P. A. Galie, K. R. Stevens, J. S. Miller, *Science* **2019**, *364*, 458 – 464; b) M.-Y. Chiang, Y.-W. Hsu, H.-Y. Hsieh, S.-Y. Chen, S.-K. Fan, *Sci. Adv.* **2016**, *2*, e1600964.

[7] Z. H. Nie, W. Li, M. Seo, S. Q. Xu, E. Kumacheva, *J. Am. Chem. Soc.* **2006**, *128*, 9408 – 9412.

[8] a) Y. Cheng, F. Y. Zheng, J. Lu, L. R. Shang, Z. Y. Xie, Y. J. Zhao, Y. P. Chen, Z. Z. Gu, *Adv. Mater.* **2014**, *26*, 5184 – 5190; b) K. Maeda, H. Onoe, M. Takinoue, S. Takeuchi, *Adv. Mater.* **2012**, *24*, 1340 – 1346; c) M. Hayakawa, H. Onoe, K. H. Nagai, M. Takinoue, *Sci. Rep.* **2016**, *6*, 20793.

[9] a) K. W. Bong, K. T. Bong, D. C. Pregibon, P. S. Doyle, *Angew. Chem. Int. Ed.* **2010**, *49*, 87 – 90; *Angew. Chem.* **2010**, *122*, 91 – 94; b) K. S. Paulsen, D. Di Carlo, A. J. Chung, *Nat. Commun.* **2015**, *6*, 6976.

[10] K. H. Roh, D. C. Martin, J. Lahann, *Nat. Mater.* **2005**, *4*, 759 – 763.

[11] S. Takeuchi, P. Garstecki, D. B. Weibel, G. M. Whitesides, *Adv. Mater.* **2005**, *17*, 1067 – 1072.

[12] a) K. W. Bong, S. C. Chapin, P. S. Doyle, *Langmuir* **2010**, *26*, 8008 – 8014; b) K. D. Seo, J. Doh, D. S. Kim, *Langmuir* **2013**, *29*, 15137 – 15141.

[13] G. S. Tang, R. H. Xiong, D. Lv, R. X. Xu, K. Braeckmans, C. B. Huang, S. C. De Smedt, *Adv. Sci.* **2019**, *6*, 1802342.

[14] M. Y. Hua, H. W. Yang, C. K. Chuang, R. Y. Tsai, W. J. Chen, K. L. Chuang, Y. H. Chang, H. C. Chuang, S. T. Pang, *Biomaterials* **2010**, *31*, 7355 – 7363.

Manuscript received: September 3, 2019
Revised manuscript received: October 27, 2019
Accepted manuscript online: November 7, 2019
Version of record online: ■■ ■■, ■■■■

Communications

Microfluidics

Z. N. Wu, Y. J. Zheng, L. Lin,* S. F. Mao, Z. H. Li, J.-M. Lin* _____ ■■■■–■■■■

Controllable Synthesis of Multicompartmental Particles Using 3D Microfluidics

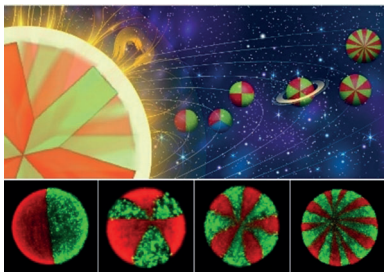

A microfluidic device, consisting of a microfluidic chip and capillary, was developed to produce multicompartmental particles. By adjusting various parameters of the device, the size of the particles and the number of different compartments within the particle could be varied. These were used to encapsulate magnetic beads, fluorescent nanoparticles, and cells.